Mature B lymphocytes accelerate wound healing after acute and chronic diabetic skin lesions

Ruxandra F. Sîrbulescu, PhD[1,2], Chloe K. Boehm[1,3], Erin Soon[1,4], Moses Q. Wilks, PhD[2,5], Iulian Ilieș, PhD[6], Hushan Yuan, PhD[2,5], Benjamin Maxner[1,7], Nicolas Chronos, MD[1], Charalambos Kaittanis, PhD[2,5], Marc D. Normandin, PhD[2,5], Georges El Fakhri, PhD[2,5], Dennis P. Orgill, MD, PhD[8], Ann E. Sluder, PhD[1], Mark C. Poznansky, MB, ChB, PhD[1,2]

[1]Vaccine and Immunotherapy Center, Division of Infectious Diseases, Department of Medicine, Massachusetts General Hospital, Boston, Massachusetts, USA. [2]Harvard Medical School, Boston, Massachusetts, USA. [3]Tufts University, Medford, Massachusetts, USA. [4]Imperial College London, London, UK. [5]Gordon Center for Medical Imaging, Nuclear Medicine and Molecular Imaging, Radiology Department, Massachusetts General Hospital, Boston, Massachusetts, USA. [6]Healthcare Systems Engineering Institute, College of Engineering, Northeastern University, Boston, Massachusetts, USA. [7]Boston University, Boston, Massachusetts, USA. [8]Division of Plastic Surgery, Brigham and Women's Hospital, Boston, Massachusetts, USA.

Correspondence should be addressed to R.F.S. (rsirbulescu@mgh.harvard.edu) or M.C.P. (mpoznansky@mgh.harvard.edu).

Supporting information

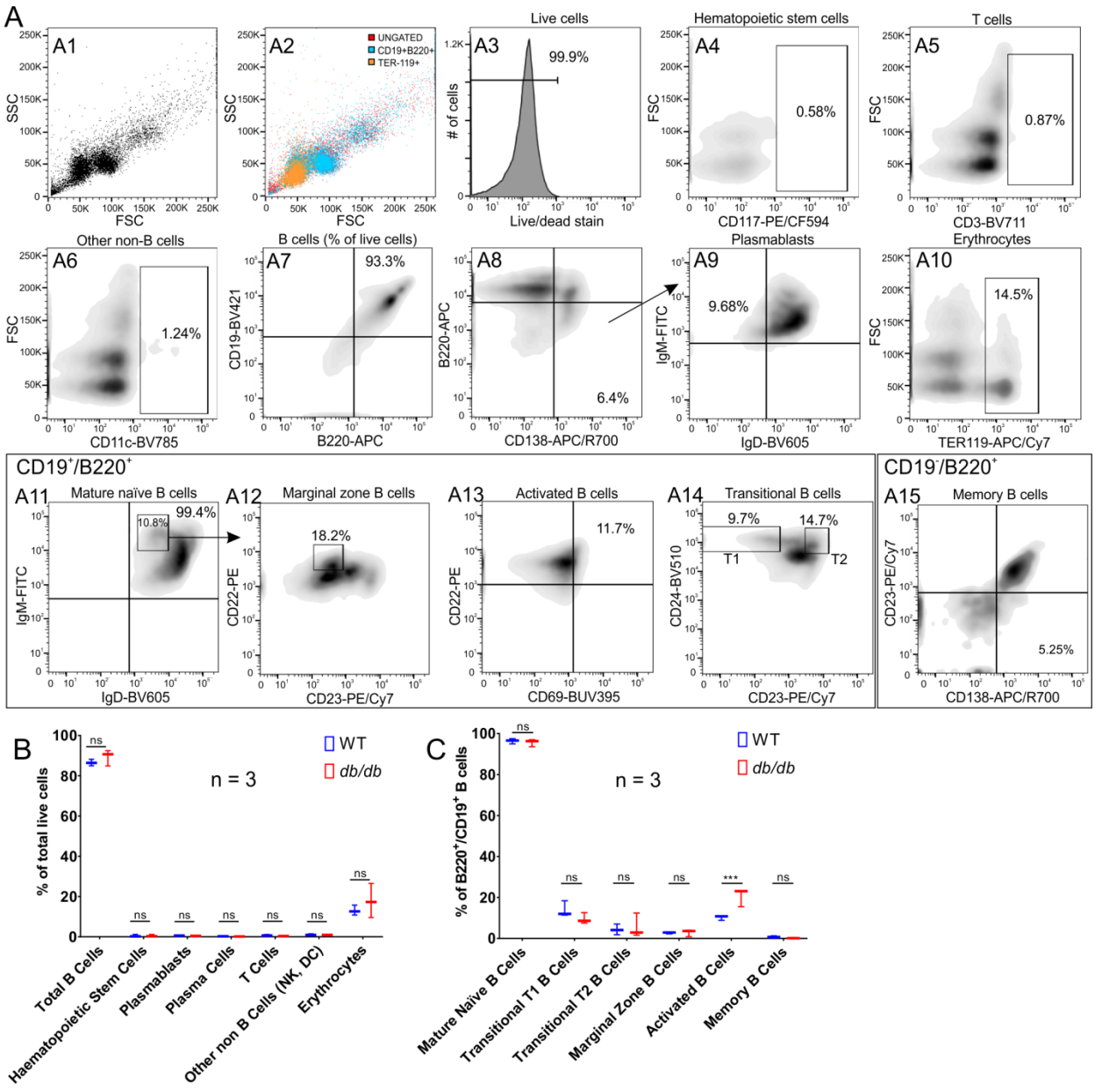

Figure S1

Flow cytometry characterization of the enriched B cell fraction applied to skin wounds. **A**. Gating strategy for the various cell categories and B cell sub-populations included in the analysis in a representative sample from WT animals. **A1**: Forward versus side scatter distribution of the enriched B cell population. **A2**: Overlay of the forward versus side scatter distributions of $CD19^{+}/B220^{+}$ B cells (blue) and TER-119+ erythrocytes, which represent the largest contaminant (yellow) over all analyzed cells (red). **A3**: Live/dead stain indicated that the majority of the cells were alive at the time of analysis. **A4-6**: The numbers of $CD117^{+}$

hematopoietic stem cells, $CD3^+$ T cells, and other non-B cell contaminants ($CD11c^+$) were practially non-detectable or present in trace numbers. Gating was performed independently, based on fluorescence-minus-one experiments for each of the analyzed markers. **A7**: In all samples, the majority of the isolated cells were $CD19^+/B220^+$ B cells. **A8-9**: A relatively small percentage of the total cell count were plasmablasts or plasma cells. **A10**: The most significant contaminant in all samples was represented by red blood cells, as indicated by TER-119 labeling. **A11-15**: Gating strategy for B cell subtypes in the enriched B cell isolate. Mature naïve B cells represented the majority of the cells (**A11**), and included marginal zone B cells (**A12**) and transitional B cells (**A14**). Very low numbers of activated B cells or memory B cells were detected in the sample illustrated (**A13, 15**). **B**. Quantitative analysis in three independent experiments performed in triplicate indicated that there was no significant difference in the proportion of B cells or contaminants between samples isolated from WT or db/db mice (n = 3 animals per genotype). **C**. Quantitative analysis showed that B cell subtypes were present in equal proportions in samples isolated from WT or db/db mice, with the exception of activated B cells, which were increased significantly in obese diabetic mice (n = 3 animals per genotype).

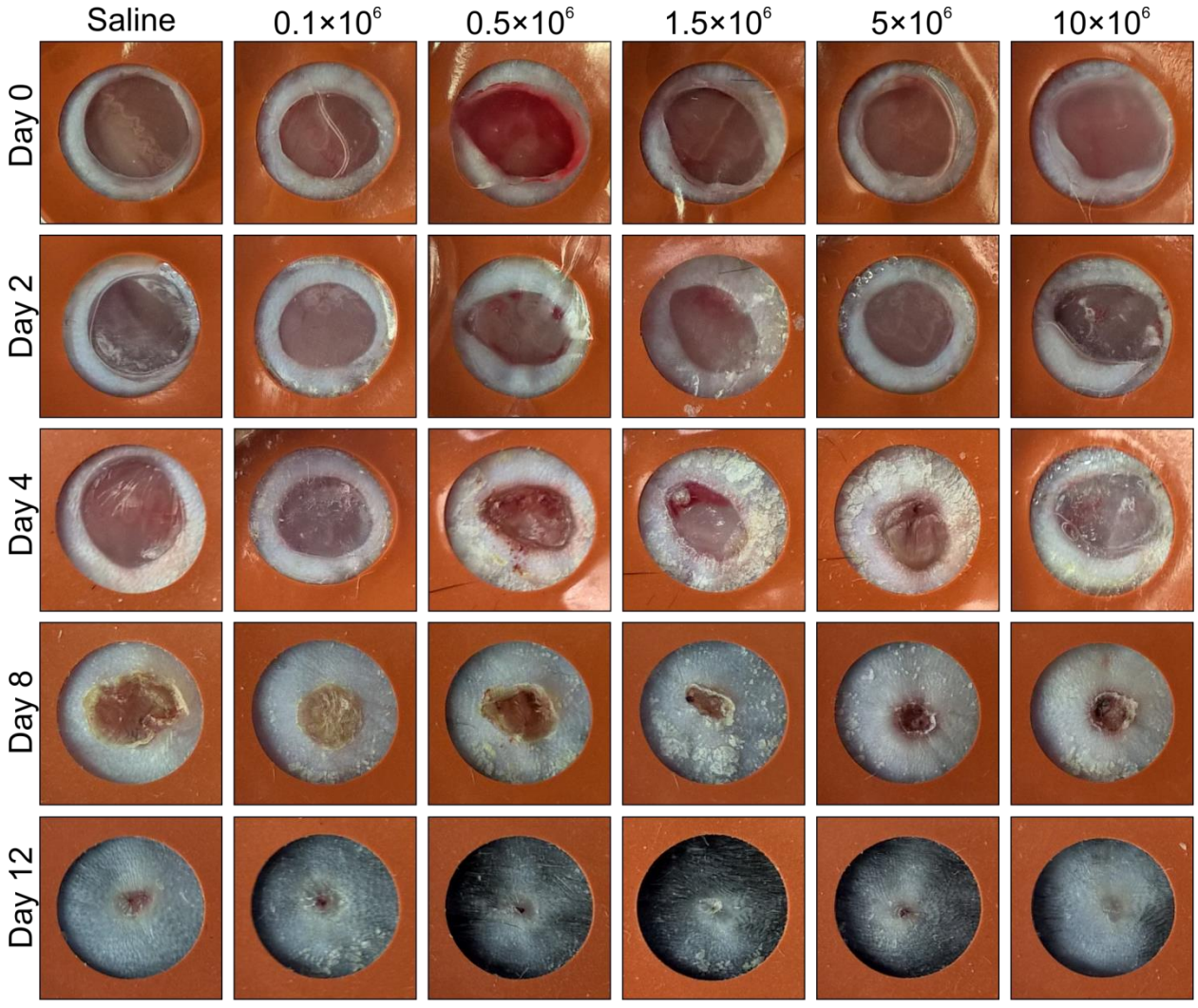
Saline
0.1×10^6
0.5×10^6
1.5×10^6
5×10^6
10×10^6
Day 0
Day 2
Day 4
Day 8
Day 12

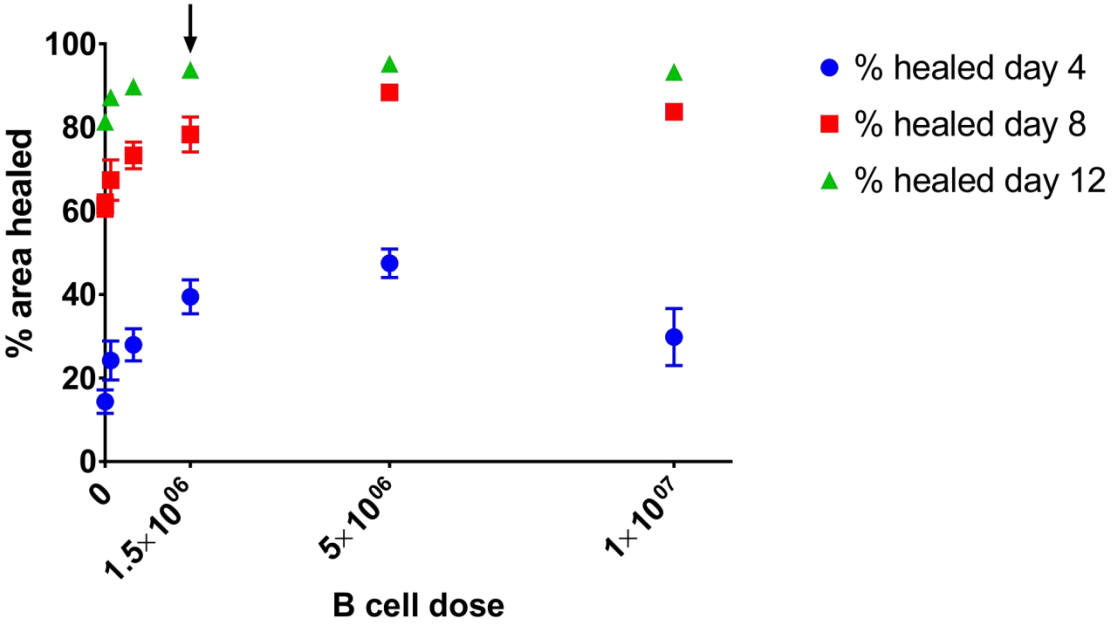
% area healed
100
80
60
40
20
0
0
1.5×10^06
5×10^06
1×10^07
B cell dose
% healed day 4
% healed day 8
% healed day 12

48

Figure S2

B cells accelerate wound healing in a dose-dependent manner. Applying B cells at different concentrations onto splinted full thickness excision lesions revealed a dose-dependent acceleration in the rate of wound closure. Increasing the amount of cells applied from 0 to 5 million per wound led to a progressively accelerated closure of the treated wounds, with the first significant improvement in the rate of wound closure as compared to saline-treated baseline observed after the application of 1.5 million cells per wound (7.5 million cells/cm^2). Further increasing the amount of applied cells to 10 million led to a slighly reduced efficacy as compared to the 1.5 and 5 million cell doses, in particular at day 4 post-injury, suggesting that the application of very high cell numbers may have detrimental effects. Interestingly, at later time points, wounds treated with the highest dose of 10 million cells performed as well as the 1.5 and 5 million cell doses. It is likely that this reflects the dynamics of the in situ cell survival, because the number of viable B exogenous cells declines rapidly after day 6 (see Fig. 5E), effectively reducing the cell numbers. For each dosage, the same wound is shown at various time points. Inner diameter of the silicone splint = 7 mm. The graph summarizes the performance of each dosage at various time points after injury examined in the course of the study (n = 6 animals per dose). Overall, the dose-response curve for B cell treatment appeared to reach a plateau beyond 1.5 million cells/wound. The latter dose was selected for subsequent wound healing experiments (arrow).

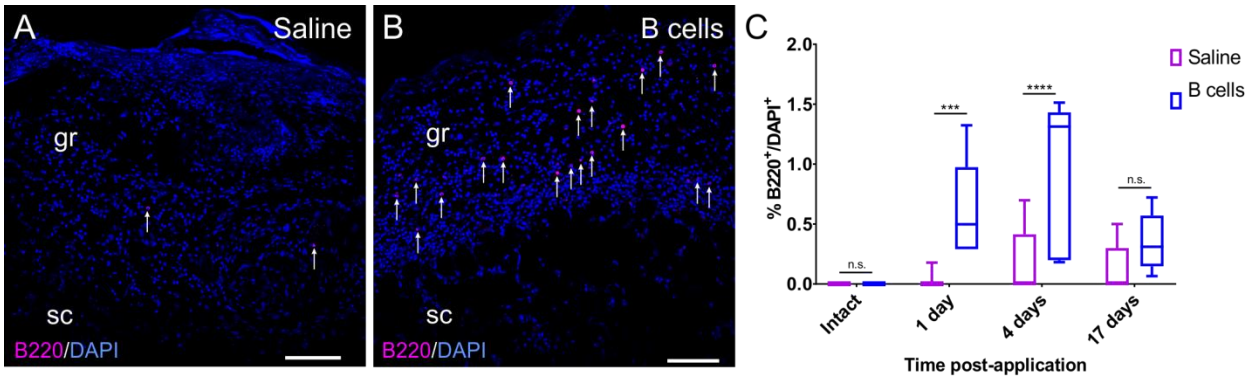

Figure S3

Immunolabeling against CD45R/B220 allows the identification of B cells in transverse sections through the wound bed. **A**. Very few B cells are normally present in the wound bed at 4 days post-injury in the granulation tissue (gr) or subcutaneous areas (sc) of the wound. Cell nuclei are counterstained with DAPI. **B**. The exogenous application of B cells leads to greatly increased numbers of B cells detectable in the wound bed 4 days after injury and treatment. Scale bars, 100 µm. **C**. Quantitative analysis of the B cell abundance in the wound bed and edges at various time points post-application. Intact, uninjured skin was analyzed for comparison. Significance was assessed using two-way ANOVA follwed by Tukey's multiple comparisons test. *** $p < 0.001$; **** $p < 0.0001$.

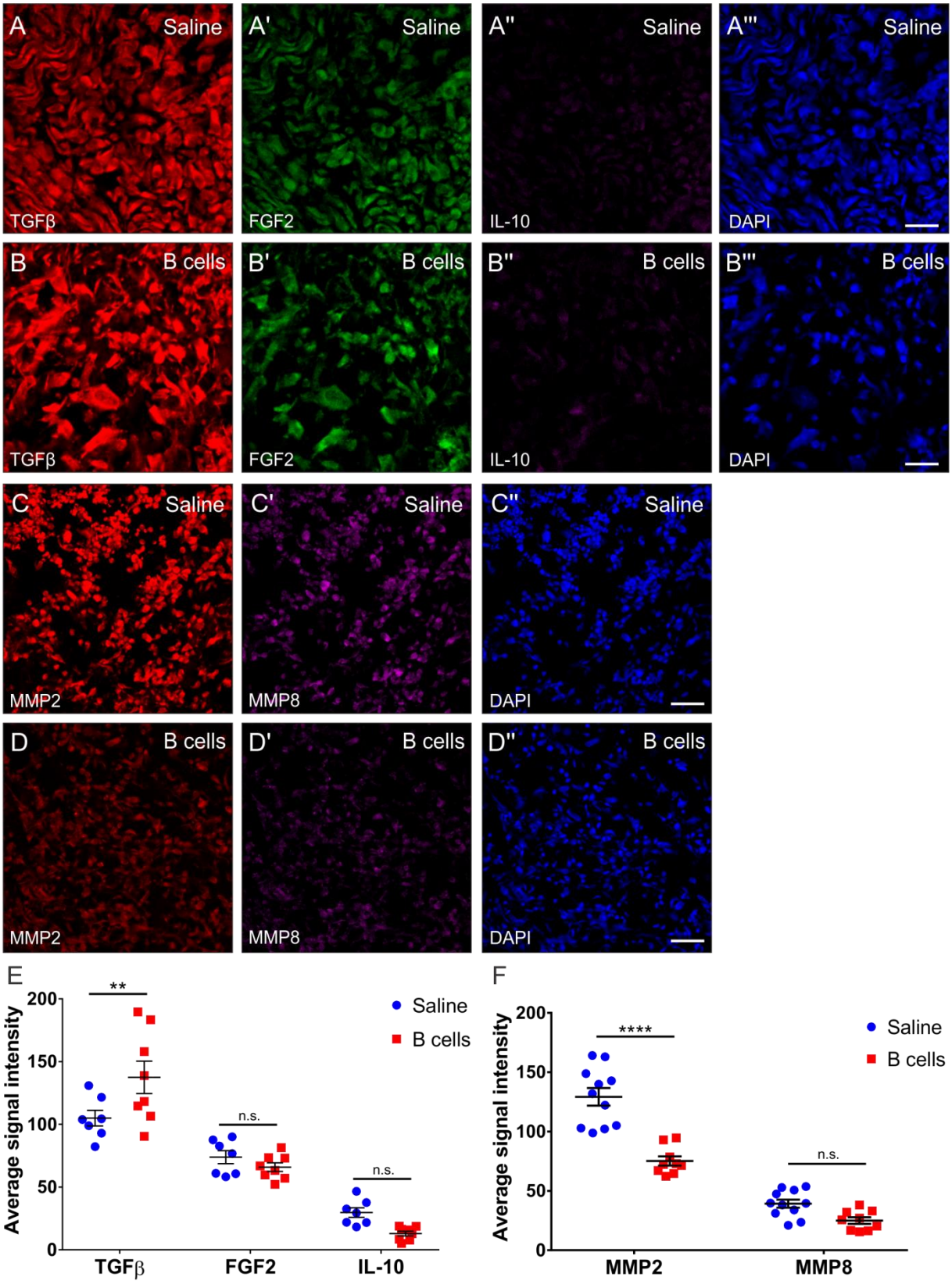
A
Saline
TGFβ
A'
Saline
FGF2
A''
Saline
IL-10
A'''
Saline
DAPI
B
B cells
TGFβ
B'
B cells
FGF2
B''
B cells
IL-10
B'''
B cells
DAPI
C
Saline
MMP2
C'
Saline
MMP8
C''
Saline
DAPI
D
B cells
MMP2
D'
B cells
MMP8
D''
B cells
DAPI
E
Average signal intensity
200
150
100
50
0
**
n.s.
n.s.
Saline
B cells
TGFβ
FGF2
IL-10
F
Average signal intensity
200
150
100
50
0
****
n.s.
Saline
B cells
MMP2
MMP8

Figure S4

B cell application alters the wound microenvironment. A-D’’’. Tissue sections collected from wound bed biopsies at 4 days post injury and treatment were immunostained for key growth factors (TGF-β, FGF2) and anti-inflammatory cytokines (IL-10), as well as major proteolytic enzymes (MMP2, MMP8). Confocal images were collected in one session, using identical parameters. **E-F**. Quantification of average intensity of the staining within cells showed a significant increase in the expression of TGF-β and a significant decrease in the expression of MMP2 in the granulation tissue of wounds that received B cell treatment at the time of injury. Statistical significance was assessed by two-way repeated-measures ANOVA, followed by Tukey’s multiple comparisons test. ** $p < 0.01$; **** $p < 0.0001$.

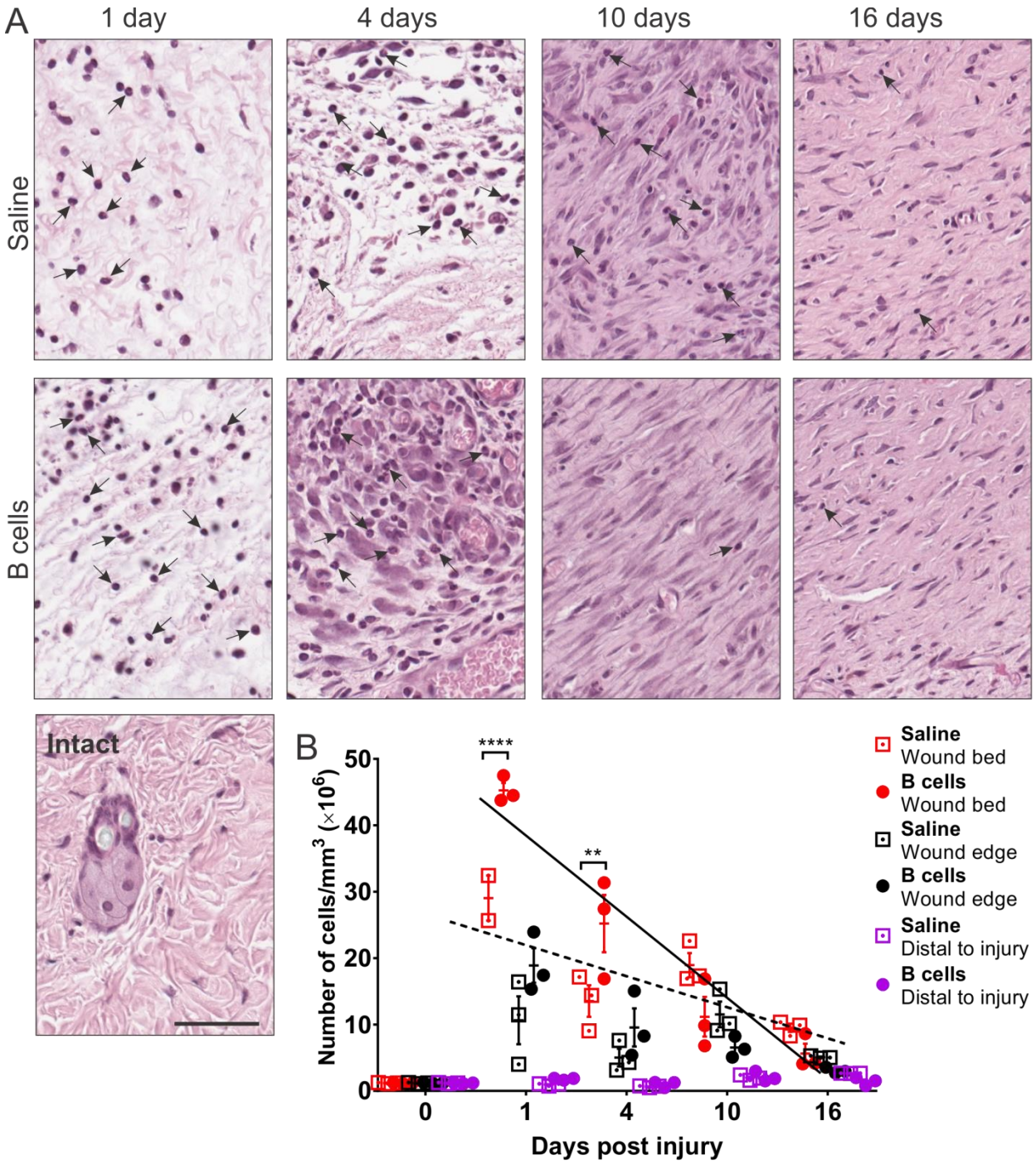

Figure S5

B cells application alters the dynamics of neutrophil infiltration after injury. **A.** Hematoxylin and eosin staining of transverse sections through the wound bed in tissue biopsies collected at various time points after injury. At early time points (1 day and 4 days), neutrophils (arrows) infiltrate the wound bed in greater numbers in wounds treated acutely with B cells. By

contrast, at later time points (10 and 16 days), the granulation and scar tissue in the wounds treated acutely with B cells had overall fewer infiltrating neutrophils. Note the denser tissue and pronounced vascularization in the granulation tissue at 4 days and the scar tissue formation at 10 days in B cell-treated wounds, suggesting accelerated progression of the wound healing. Scale bar, 50 μm. **B**. Quantitative analysis of neutrophil infiltration in the wound bed, edges, and distal to the wound site. Neutrophils were present in very low numbers in intact tissue (0 time point) or at distal locations, >3 mm away from the wound edge. In the wound bed, neutrophil infiltration was most pronounced at 1 day after injury, and it was significantly higher in B cell-treated wounds as compared to saline-treated controls. The numbers of infiltrating neutrophils decreased rapidly over time, moreso in B cell-treated wounds. While the regression line slope of the saline-treated controls (dashed line) was -5.3, in the B cell-treated wounds it reached -13.3 (continuous line), indicating a 2.5-fold increase in the rate of decay of cell numbers. Neutrophil infiltration into the wound edges followed a similar trend as the wound bed, with B cell-treated wounds showing a peak in cell numbers at 1 day post injury as compared to saline-treated wounds where the maximum cell infiltration was delayed until day 10 after injury.

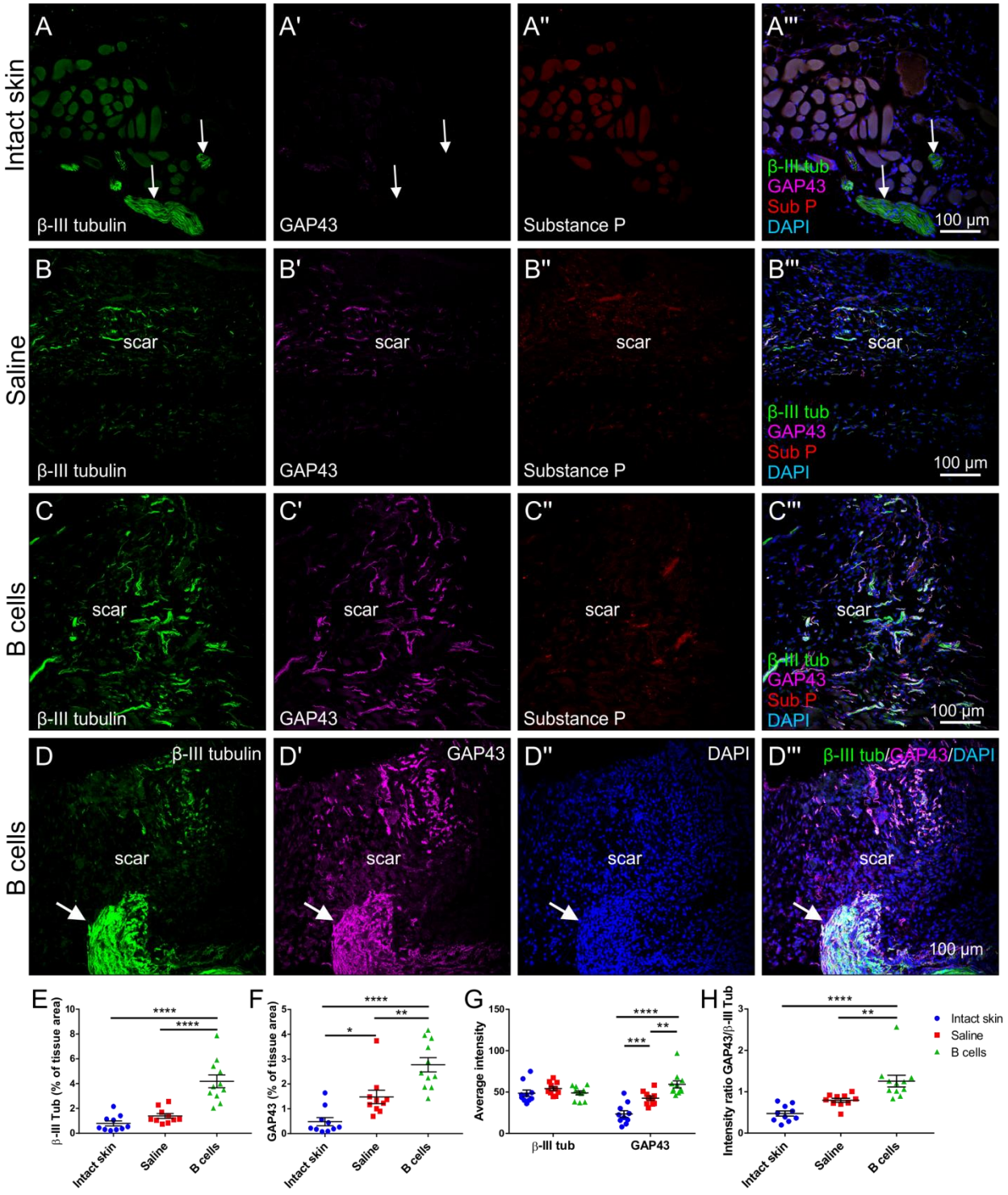

Figure S6

B cell application at the time of injury is associated with increased regenerative capacity of the nerve fibers in the scar tissue. A-A'''. Confocal images of transverse sections through intact skin tissue showing cutaneous nerves (arrows) immunolabeled against β-III tubulin, with

minimal expression of GAP43 or substance P. **B-B'''**. Similar immunolabeling in tissue sections collected from biopsies at 16 days post-injury in a saline treated (control) animal reveals innervation of the scar tissue. The newly growing nerve endings show GAP43 expression but lack substance P. **C-C'''**. In wounds that were treated with B cells at the time of injury, numerous nerve endings expressing both β-III tubulin and GAP43 but not substance P can be observed. **D-D'''**. Typical example of cutaneous nerve growth immediately under the scar tissue and numerous fine nerve endings invading the scar tissue in B cell-treated tissues. Note that GAP43 is strongly expressed even in the distant axons of the cutaneous nerve (arrow). Such instances were rarely observed in biopsies derived from saline-treated wounds. **E**. Replicating previous experiments, the area covered by β-III tubulin+ immunostaining was significantly increased in B cell treated wounds. **F**. The area covered by $GAP43^{+}$ fibers was significantly increased in tissues treated with B cells as compared to either saline-treated or intact control, while saline-treated wounds did show a significant increase in GAP43 immunolabeling as compared to uninjured tissue. **G**. The average intensity of the staining within all detected nerve endings was similar between experimental conditions for β-III tubulin, but showed significant differences for GAP43, with B cell-treated tissues showing the highest GAP43 immunolabeling intensity. **H**. The ratio of GAP43/ β-III tubulin, which served as a measure of the regenerative capacity of axons, was significantly higher in B cell treated tissue as compared to either saline-treated wounds or intact tissue. Statistical significance was assessed by one-way ANOVA, followed by Tukey's multiple comparisons test. * $p < 0.05$; ** $p < 0.01$; *** $p < 0.001$; **** $p < 0.0001$.

Table S1: Characterization of the cellular composition of enriched B cell isolate from spleen.

Cell type	Characteristic markers	WT spleen (average % of total ± SEM) n = 3	db/db spleen (average % of total ± SEM) n = 3
B cells	$B220^{+}$ $CD19^{+}$	86.5 ± 0.93	89.4 ± 2.29
Hematopoietic stem cells	$CD117^{+}$	0.48 ± 0.34	0.51 ± 0.32
Plasmablasts	$B220^{low}CD138^{+}$	0.62 ± 0.10	0.39 ± 0.10
Plasma cells	$B220^{-}CD138^{+}$	0.22 ± 0.04	0.11 ± 0.03
T cells	$CD3^{+}B220^{-}CD19^{-}$	0.71 ± 0.21	0.37 ± 0.04
Other non-B cells (NK, DC)	$CD11c^{+}$	1.05 ± 0.20	0.89 ± 0.10
Erythrocytes	$TER\text{-}119^{+}$	13.0 ± 1.43	17.8 ± 4.89

Table S2: Characterization of the B cell subpopulations in the enriched isolate applied to wounds.

B cell subtype	Characteristic markers (gated on $B220^+/CD19^+$)	WT spleen (average % of $B220^+/CD19^+$ cells ± SEM) n = 3	db/db spleen (average % of $B220^+/CD19^+$ cells ± SEM) n = 3
Mature Naïve B Cells	IgM^+IgD^+	96.4 ± 0.73	95.6 ± 1.04
Transitional T1 B Cells	$IgM^+IgD^+CD24^+CD23^-$	13.93 ± 2.24	9.57 ± 1.55
Transitional T2 B Cells	$IgM^+IgD^+CD24^+CD23^{high}$	4.31 ± 1.50	5.62 ± 3.41
Marginal Zone B Cells	$IgM^{high}IgD^{low}CD22^{high}CD23^-$	2.73 ± 0.25	2.84 ± 0.98
Activated B Cells	$CD69^+$	10.18 ± 0.66	20.6 ± 2.55
Memory B Cells	$CD138^+CD23^-$	0.68 ± 0.36	0.19 ± 0.12

Table S3: Wound scoring criteria and range.

Parameter	Score 1	2	3	4
Presence of granulation tissue	Abundant	Moderate	Low	Absent
Collagen fiber orientation	Vertical	Mixed	Horizontal	-
Maturity of collagen	Mostly immature (%B/RGB <40%)	Intermediate (%B/RGB= 40-50%)	Mostly mature (%B/RGB >50%)	-
Pattern of collagen deposition	Densely packed fascicles	Mixed fascicle and reticular	Reticular	-
Angiogenesis	Absent	Low (1-9 capillaries/ 500 μm^2)	Moderate (10-15 capillaries/ 500 μm^2)	High (>15 capillaries/ 500 μm^2)
Thickness of regenerated tissue	Thin (<500 µm in WT) (<100 µm in *db/db*)	Moderate (500-1000 µm in WT) (100-200 µm in *db/db*)	Thick (>1000 µm in WT) (>200 µm in *db/db*)	-
Width of scar	Wide (>1000 µm in WT) (>2000 µm in *db/db*)	Moderate (600-1000 µm in WT) (1500-2000 µm in *db/db*)	Narrow (<600 µm in WT) (<1500 µm in *db/db*)	-
Regenerated structures (e.g. nerve endings)	Absent	Present	-	-